

Multireference Ab Initio Calculations on Reaction Intermediates of the Multicopper Oxidases

Jakub Chalupský,[†] Frank Neese,[‡] Edward I. Solomon,[§] Ulf Ryde,^{||} and Lubomír Rulíšek^{*†}

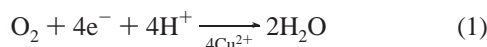
Institute of Organic Chemistry and Biochemistry, Academy of Sciences of the Czech Republic, and Gilead Sciences Research Center at IOCB, Flemingovo nám. 2, 166 10 Praha 6, Czech Republic, Department of Theoretical Chemistry, Lund University, Chemical Center, P.O. Box 124, S-221 00 Lund, Sweden, Department of Chemistry, Stanford University, Stanford, California 94305, and Institut für Pysikalische und Theoretische Chemie, Universität Bonn, Wegelerstrasse 12, D-53115 Bonn, Germany

Received October 12, 2006

The multicopper oxidases (MCOs) couple the four-electron reduction of dioxygen to water with four one-electron oxidations of various substrates. Extensive spectroscopic studies have identified several intermediates in the MCO catalytic cycle, but they have not been able to settle the structures of three of the intermediates, viz. the native intermediate (NI), the peroxy intermediate (PI), and the peroxy adduct (PA). The suggested structures have been further refined and characterized by quantum mechanical/molecular mechanical (QM/MM) calculations. In this paper, we try to establish a direct link between theory and experiment, by calculating spectroscopic parameters for these intermediates using multireference wave functions from the multistate CASPT2 and MRDDCI2 methods. Thereby, we have been able to reproduce low-spin ground states ($S = 0$ or $S = 1/2$) for all the MCO intermediates, as well as a low-lying ($\sim 150\text{ cm}^{-1}$) doublet state and a doublet–quartet energy gap of $\sim 780\text{ cm}^{-1}$ for the NI. Moreover, we reproduce the zero-field splitting ($\sim 70\text{ cm}^{-1}$) of the ground 2E state in a D_3 symmetric hydroxy-bridged trinuclear Cu(II) model of the NI and obtain a quantitatively correct quartet–doublet splitting (164 cm^{-1}) for a μ_3 -oxo-bridged trinuclear Cu(II) cluster. All results support the suggestion that the NI has an O^{2-} atom in the center of the trinuclear cluster, whereas both the PI and PA have an O_2^{2-} ion in the center of the cluster, in agreement with the QM/MM results and spectroscopic measurements.

1. Introduction

The multicopper oxidases (MCO) couple four one-electron oxidations of a substrate with the four-electron reduction of molecular oxygen to water:^{1,2}



The most studied members of this family are laccase (Lc),^{3,4} ascorbate oxidase (AO),⁵ ceruloplasmin (Cp),⁶ Fet3p (along

with Cp exhibiting ferroxidase activity),⁷ and CueO (part of the copper regulation system).⁸

All known MCOs contain at least four copper ions, denoted according to their spectroscopic characteristics as type 1 (T1), type 2 (T2), and type 3 (T3). The type 1 copper ion (Cu1) is located at the substrate-binding site and is coordinated to one cysteine (Cys) and two histidine (His) residues. In most structures, it also binds to a fourth weak axial ligand, typically methionine. It exhibits a strong absorption band around 600 nm arising from a $S_{Cys} \rightarrow Cu^{II}$ charge-transfer excitation, which gives rise to the intense blue

* To whom correspondence should be addressed. E-mail: rulisek@uochb.cas.cz. Phone (fax): +420-220-183-263(299).

[†] Academy of Sciences of the Czech Republic.

[‡] Bonn University.

[§] Stanford University.

^{||} Lund University.

(1) Messerschmidt, A. In *Multicopper oxidases*; Messerschmidt, A., Ed.; World Scientific: Singapore, River Edge, NJ, 1997; pp 23–80.

(2) Solomon, E. I.; Sundaram, U. M.; Machonkin, T. E. *Chem. Rev.* **1996**, *96*, 2563–2605.

(3) Xu, F. *Biochemistry* **1996**, *35*, 7608–7614.

(4) Davies, G. J.; Ducros, V. In *Handbook of Metalloproteins*; Messerschmidt, A., Huber, R., Wieghardt, K., Poulos, T., Eds.; Wiley: New York, 2001; pp 1359–1368.

(5) Malkin, R.; Malmström, B. G. *Adv. Enzymol.* **1970**, *33*, 177–243.

(6) Crichton, R. R.; Pierre, J.-L. *BioMetals* **2001**, *14*, 99–112.

(7) de Silva, D. M.; Askwith, C. C.; Eide, D.; Kaplan, J. J. *Biol. Chem.* **1995**, *270*, 1098–1101.

(8) Outten, F. W.; Huffman, D. L.; Hale, J. A.; O'Halloran, T. V. *J. Biol. Chem.* **2001**, *276*, 30670–30677.

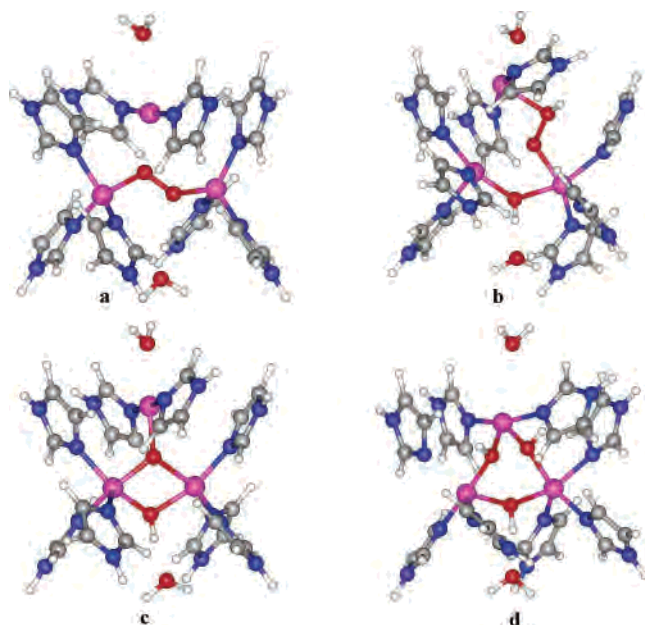


Figure 1. Structural models of the peroxy (PI) and native (NI) intermediates as suggested by spectroscopic measurements and QM/MM calculations: (a) PI_C; (b) PI_S; (c) NI_C; (d) NI_S.^{12,14,21}

color of the copper oxidases. The type 2 copper ion (Cu²) is located at one vertex of a trinuclear copper cluster (cf. Figure 1). It is bound to two His residues from the protein and to a solvent molecule, which is OH⁻.⁹ The two T3 copper ions have three His ligands each and are bridged by a solvent molecule in the oxidized state. They form an antiferromagnetically coupled pair and show a characteristic 330 nm absorption band arising from an OH⁻ → Cu^{II} charge-transfer transition.¹⁰ The four electrons necessary for the reduction of dioxygen are shuttled from Cu^I to the trinuclear cluster, where the reduction of O₂ takes place. The two sites are connected by a His–Cys–His peptide link (where Cys is a ligand of Cu^I and each of the two His residues is bound to one of the two T3 copper ions), which span a Cu–Cu distance of ~13 Å.

Detailed mechanistic information has been provided by a number of spectroscopic techniques.^{11–16} Specifically, two intermediates—peroxy intermediate (PI¹¹) and native intermediate (NI¹⁴)—have been observed. PI has been best characterized as the peroxide moiety bound in the trinuclear (Cu^I)(Cu^{II})₂ T2–T3 copper (i.e., two electrons have been transferred from the copper ions in the fully reduced state

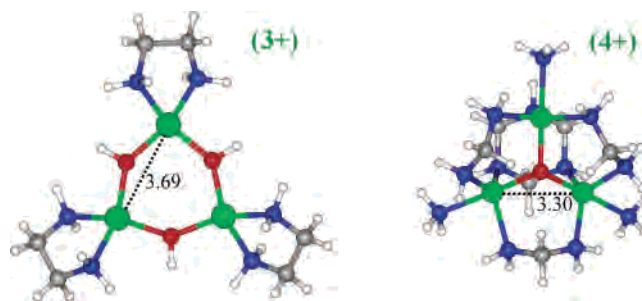


Figure 2. Structures of the TrisOH and the μ_3 -O complexes, models of the NI_S and NI_C binding modes of the native intermediate. Experimental spectra have recently been reported for these two models.^{17,19,20} The TrisOH complex actually contained six *tert*-butyl groups (one on each nitrogen atom), but these have been truncated to hydrogens in our model. The net charges of the complexes are +3 and +4, respectively.

to incoming dioxygen molecule). It has an $S = 0$ ground state. Further, the NI has been shown to be a four-electron-reduced hydroxide product of the O–O bond cleavage, bound to a fully oxidized trinuclear cluster.¹⁴ It has a total spin of 1/2 and shows electronic coupling over all three copper ions in the trinuclear cluster. The NI decays to the resting oxidized state, but this process is so slow that it is believed that it is the NI, and not the oxidized resting state, that is the catalytically relevant fully oxidized form of the enzyme.¹⁴

For both NI and PI, two different structural models are compatible with the spectroscopic studies. One suggestion of the PI has O₂²⁻ bound in the center of the trinuclear cluster, with one oxygen atom coordinated to Cu² and the other binding between the two T3 Cu ions (PI_C; Figure 1a). The other alternative has a HO₂⁻ ion at the periphery of the trinuclear cluster, with the unprotonated oxygen atom bridging between Cu² and one of the two T3 Cu ions (PI_S; Figure 1b). Likewise, one possible model for the NI contains an O²⁻ ion in the center of the trinuclear cluster, coordinating to all three Cu ions (NI_C; Figure 1c). The other alternative has three OH⁻ ions (two from a complete reduction of O₂), each bridging two of the Cu ions in the trinuclear cluster (NI_S; Figure 1d).

Therefore, two possible inorganic models of the NI have been synthesized and studied experimentally, a 3-fold D_3 -symmetric trinuclear tris(μ -hydroxy)tricopper(II) cluster (TrisOH) and a C_3 -symmetric μ_3 -oxo-bridged trinuclear Cu(II) model (μ_3 O), depicted in Figure 2.^{17–20}

Comparative variable-temperature, variable-field MCD studies indicated that the latter structure is the best model of the native intermediate.²⁰

Recently, a detailed QM/MM (combined quantum mechanics and molecular mechanics) study was published, based on the crystal structure of CueO at 1.4 Å resolution.²¹ In this, all the four structural alternatives of the NI and PI could be obtained (Figure 1), but the energies indicated that PI is most stable with the peroxide in the center of the cluster

- (9) Quintanar, L.; Yoon, J.; Aznar, C. P.; Palmer, A. E.; Andersson, K. K.; Britt, R. D.; Solomon, E. I. *J. Am. Chem. Soc.* **2005**, *127*, 13832–13845.
- (10) Spira-Solomon, D. J.; Solomon, E. I. *J. Am. Chem. Soc.* **1987**, *109*, 6421–6432.
- (11) Shin, W.; Sundaram, U. M.; Cole, J. L.; Zhang, H. H.; Hedman, B.; Hodgson, K. O.; Solomon, E. I. *J. Am. Chem. Soc.* **1996**, *118*, 3202–3215.
- (12) Palmer, A. E.; Lee, S.-K.; Solomon, E. I. *J. Am. Chem. Soc.* **2001**, *123*, 6591–6599.
- (13) Palmer, A. E.; Quintanar, L.; Severance, S.; Wang, T.-P.; Kosman, D. J.; Solomon, E. I. *Biochemistry* **2002**, *41*, 6438–6448.
- (14) Lee, S.-K.; George, S. D.; Antholine, W. E.; Hedman, B.; Hodgson, K. O.; Solomon, E. I. *J. Am. Chem. Soc.* **2002**, *124*, 6180–6193.
- (15) Torres, J.; Svistunenko, D.; Karlsson, B.; Cooper, C. E.; Wilson, M. T. *J. Am. Chem. Soc.* **2002**, *124*, 963–967.
- (16) Solomon, E. I.; Chen, P. I.; Metz, M.; Lee, S.-K.; Palmer, A. E. *Angew. Chem., Int. Ed.* **2001**, *40*, 4570–4590.

- (17) Yoon, J.; Mirica, L. M.; Stack, T. D. P.; Solomon, E. I. *J. Am. Chem. Soc.* **2004**, *126*, 12586–12595.
- (18) Mirica, L. M.; Stack, T. D. P. *Inorg. Chem.* **2005**, *44*, 2131–2133.
- (19) Yoon, J.; Solomon, E. I. *Inorg. Chem.* **2005**, *44*, 8076–8086.
- (20) Yoon, J.; Mirica, L. M.; Stack, T. D. P.; Solomon, E. I. *J. Am. Chem. Soc.* **2005**, *127*, 13680–13693.
- (21) Rulíšek, L.; Solomon, E. I.; Ryde, U. *Inorg. Chem.* **2005**, *44*, 5612–5628.

(PI_C; Figure 1a). Likewise, the NI most likely corresponds to the μ_3 -oxo-bridged structure (NI_C), depicted in Figure 1c.

In summary, the combination of spectroscopic techniques and QM/MM calculations has led to a structural characterization of the intermediates in the reaction cycle of MCO. Despite all these achievements, some uncertainty still remains concerning the details of the reaction mechanism of O₂ reduction in MCOs. First, the spectroscopic data provide detailed insight into the electronic structures of the intermediates and these should be correlated to the calculations. Second, DFT methods were used for the description of the quantum system in the QM/MM study. This is the method of choice for model bioinorganic systems comprising up to ~200 atoms, but it suffers from known deficiencies, such as a less accurate treatment of spin states with a multireference character and the overestimation of the electron delocalization, especially for mixed-valence states.^{22,23} This may lead to errors of ~25 kJ·mol⁻¹ in spin states splitting energies.²⁴ Also, since many low-spin states are broken-symmetry solutions with the eigenvalue of \hat{S}^2 deviating significantly from what is expected for the pure spin states, the use of spin projection techniques is a necessary to obtain physically correct properties. Thus, the triplet state ($S = 1$) was predicted to be lower in energy than singlet state ($S = 0$) for the most plausible model of the PI (formally in the Cu^ICu^{II}₂ oxidation state), in contrast to experiments,¹¹ which has been the major problem in the otherwise unambiguous structural assignment.²¹

In this study, we attempt to provide a direct link to the experimental results by calculating spectroscopic parameters of the QM/MM protein structures by correlated multireference methods (CASPT2, MRDDCI2) with the inclusion of spin-orbit coupling (SOC). Concomitantly, the methods are carefully tested on the two inorganic Cu₃ models of the NI.^{17–20} These calculations have enabled us to characterize the nature of the ground and excited electronic states, to further support the assignment of structures to the observed intermediates, and to discuss the reaction mechanism of the MCOs.

2. Computational Details

Multireference CASPT2/CASSCF and RAS-SI Calculations.

All the multireference calculations, i.e., the complete active space self-consistent field (CASSCF),²⁵ complete active space second-order perturbation theory (CASPT2),²⁶ and multistate CASPT2 (MS-CASPT2) calculations, were carried out with the MOLCAS 6.0 program suite.²⁷ Throughout, the ANO-S basis set (contracted as [6s4p3d2f] for Cu, [3s2p1d] for O and N, and [2s] for H) has been used.²⁸

The computational protocol consisted of several steps: (i) state-specific calculations of the ground states (singlets for the PI and doublets for the other systems) and the lowest excited states of higher multiplicities (triplets and quartets), followed by CASPT2 calculations; (ii) state-averaged calculations of the first four excited states of both multiplicities for the NI, PI, and PA (an analog of PI with all three Cu's oxidized; vide infra), and the oxidized resting state, followed by MS-CASPT2; (iii) calculations of the spin-orbit coupling (SOC) among all the states calculated in previous step using the RAS-SI (restricted active space-state interactions) program.²⁹ To improve the accuracy of the spin-orbit state energies, CASPT2 energies were used in the main diagonal of the spin-orbit interaction matrix. These calculations were carried out only for systems for which experimental data are known, in an effort to obtain a direct comparison between theory and experiment.

For all systems, the active space in the CASSCF calculations comprised all d electrons in the occupied d orbitals of the three copper atoms, i.e., 15 orbitals containing 27 or 28 d electrons (depending on the redox state of the copper cluster). Since four of the five d orbitals on each copper atom are essentially doubly occupied, we also tested calculations with three electrons in three active orbitals. This did not lead to any significant difference in the description of the lowest states, so we can conclude that a CASSCF(3,3) calculation is quantitatively sufficient for the description of the low-lying quartet and doublet states that can be obtained within this small active space. However, since the calculations with the larger active space could be done at essentially identical computational cost, all the reported results have been obtained with larger active space. In all CASSCF calculations, a level shift of 1.5 to 4.5 a.u. was used to improve the convergence of the multireference wave function. In the CASPT2 calculations, an imaginary level shift of 0.2 a.u. was used to eliminate intruder states.

MRDDCI2 Calculations. In addition to the CASPT2 calculations, multireference difference dedicated CI calculations with up to two degrees of freedom (MRDDCI2)^{30,31} were performed on top of a CASSCF(3,3) reference wave functions. The calculations were carried out with the TZVP basis set on Cu and SV(P) on all other atoms.³² The MRDDCI2 calculations were of the individually selecting type using a configuration selection threshold of 10⁻⁷ au. These calculations were done with the ORCA program.³³

DFT Calculations. Density functional theory (DFT) and time-dependent DFT (TD-DFT) calculations were carried out with the Turbomole 5.7 software.³⁴ Two functionals have been used: Becke-Perdew86 (BP86),³⁵ expedited by expanding the Coulomb interactions in an auxiliary basis set, the resolution-of-identity (RI) approximation,^{36,37} and Becke's three-parameter hybrid functional B3LYP,³⁸ as implemented in Turbomole.³⁹ These calculations

- (22) Barone, V.; Bencini, A.; Ciofini, I.; Daul, C. A.; Totti, F. *J. Am. Chem. Soc.* **1998**, *120*, 8357–8365.
- (23) Lundberg, M.; Siegbahn, P. E. M. *J. Chem. Phys.* **2005**, *122*, Art. No. 224103.
- (24) Reiher, M.; Salomon, O.; Hess, B. A. *Theor. Chem. Acc.* **2001**, *107*, 48–55. Reiher, M. *Inorg. Chem.* **2002**, *41*, 6928–6935.
- (25) Roos, B. O.; Taylor, P. R. *Chem. Phys.* **1980**, *48*, 157–173.
- (26) Andersson, K.; Malmqvist, P.-Å.; Roos, B. O. *J. Chem. Phys.* **1992**, *96*, 1218–1226.
- (27) Karlström, G.; Lindh, R.; Malmqvist, P.-Å.; Roos, B. O.; Ryde, U.; Veryazov, V.; Widmark, P.-O.; Cossi, M.; Schimmelpfennig, B.; Neogrady, P.; Seijo, L. *Comput. Mater. Sci.* **2003**, *28*, 222–239.
- (28) Pierflout, K.; Dumez, B.; Widmark, P.-O.; Roos, B. O. *Theor. Chim. Acta* **1995**, *90*, 87–114.

- (29) Malmqvist, P.-Å.; Roos, B. O.; Schimmelpfennig, B. *Chem. Phys. Lett.* **2002**, *357*, 230–240.
- (30) Neese, F. *J. Chem. Phys.* **2003**, *119*, 9428–9443.
- (31) Miralles, J.; Castell, O.; Caballol, R.; Malrieu, J. P. *Chem. Phys.* **1993**, *172*, 33–43.
- (32) Schäfer, A.; Horn, H.; Ahlrichs, R. *J. Chem. Phys.* **1992**, *97*, 2571–2577.
- (33) Neese, F. *ORCA-An ab initio, Density Functional and Semiempirical program package*, version 2.4; Max-Planck-Institut für Bioorganische Chemie: Mülheim an der Ruhr, Germany, 2004.
- (34) Treutler, O.; Ahlrichs, R. *J. Chem. Phys.* **1995**, *102*, 346–354.
- (35) (a) Becke, A. D. *Phys. Rev. A* **1988**, *38*, 3098–3100. (b) Perdew, J. P. *Phys. Rev. B* **1986**, *33*, 8822–8824.
- (36) Eichkorn, K.; Treutler, O.; Öhm, H.; Häser, M.; Ahlrichs, R. *Chem. Phys. Lett.* **1995**, *240*, 283–289.
- (37) Eichkorn, K.; Weigen, F.; Treutler, O.; Ahlrichs, R. *Theor. Chem. Acc.* **1997**, *97*, 119–124.
- (38) (a) Lee, C. T.; Yang, W. T.; Parr, R. G. *Phys. Rev. B* **1988**, *37*, 785–789. (b) Becke, A. D. *J. Chem. Phys.* **1993**, *98*, 5648–5652. (c) Stephens, P. J.; Devlin, F. J.; Chabalowski, C. F.; Frisch, M. J. *J. Phys. Chem.* **1994**, *98*, 11623–11627.
- (39) Hertwig, R. H.; Koch, W. *Chem. Phys. Lett.* **1997**, *268*, 345–351.

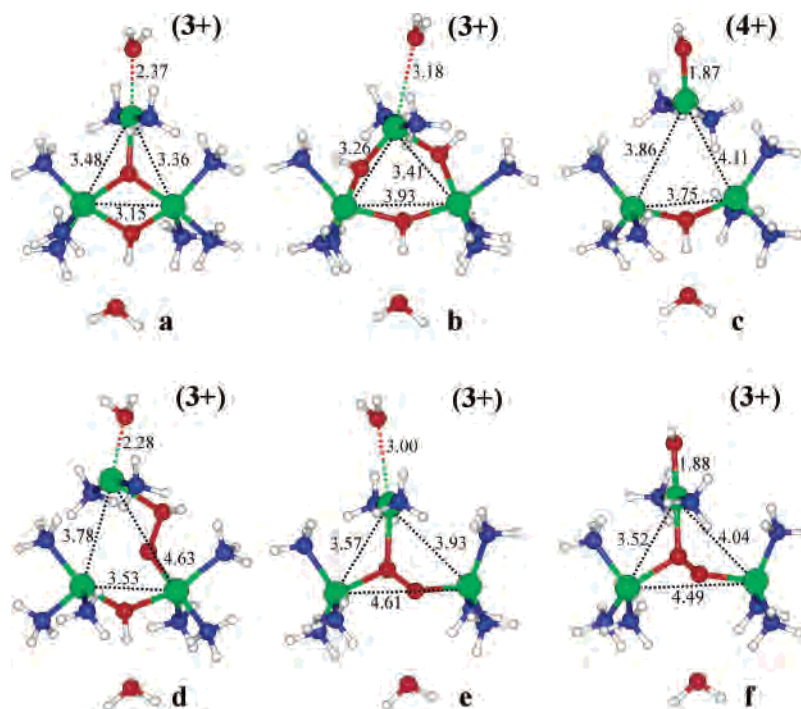


Figure 3. Six models of possible intermediates in the reaction cycle of the MCOs studied in this investigation, the native intermediate in the Ni_C (a) and Ni_S (b) binding modes, the oxidized resting state (c), the peroxy intermediate in the Pi_S (d) and Pi_C (e) binding modes, and the noncatalytic peroxy adduct in the Pa_C binding mode (f). All distances are in Å. The total charges of the studied complexes are denoted as well.

employed the 6-311+G(2d,2p) basis set⁴⁰ on all atoms except Cu, for which the DZP basis set of Schäfer et al. was used, enhanced with s-, p-, d-, and f-type functions with coefficients 0.0155 (s), 0.174 (p), 0.046199 (p), 0.132 (d), 0.39 (f), and 3.55 (f).^{41,42} Both ferromagnetically ($S = 3/2$ or 1) and antiferromagnetically coupled states ($S = 1/2$ or 0) were studied.⁴³ The broken-symmetry approach was employed to obtain the low-spin states.⁴⁴

Model Systems. In this investigation, we have studied the TrisOH and $\mu_3\text{O}$ model complexes that represent models of the two alternative binding models of the NI and have been studied experimentally (Figure 2).^{16–19} In addition, six QM/MM models of MCO intermediates were considered in this study. The latter ones are shown in Figure 3. It can be seen that, in all of them, the histidine side chains were represented by NH_3 ligands (to save computer time in these very time-consuming calculations; the results

of these calculations²¹ justify this approximation a posteriori). We included two models for the NI (which is in the Cu^{II} redox state), viz. either with O^{2-} in the center of the cluster and OH^- as a bridging ligand (Ni_C, Figure 3a) or with three OH^- ligands bridging each of three Cu–Cu pairs (Ni_S, Figure 3b). Both models have water as the Cu₂ ligand. In addition, the consensus model of the resting oxidized state (Ox, Figure 3c, also in the Cu^{II} state) was considered, with OH^- both as the Cu₂ and bridging ligand. Two models were tested for the PI, viz. either with O_2^{2-} binding in the center of the trinuclear cluster (Pi_C, Figure 3e) or with HO_2^- binding on the side between Cu₂ and one T3 copper ion (Pi_S, Figure 3d). Both models have a water ligand on Cu₂ and the Pi_S model has also a bridging OH^- ligand between the two T3 ions. These intermediates are in the formal $\text{Cu}^{\text{I}}\text{Cu}^{\text{II}}$ redox state. Finally, a model similar to the Pi_C was also used for the peroxy adduct (PA, Figure 3f), i.e., with the same atoms but in the Cu^{II} redox state. PA is not a catalytic intermediate, instead it is formed upon the addition of peroxide to the Ox state. This state has also been spectroscopically characterized,⁴⁵ and it played a major role in the discussions about the nature of the PI,²¹ because it shares most of spectroscopic characteristics with the PI. The excellent agreement of the Pi_C and Pa_C QM/MM structures (especially the Cu–Cu distances, which are very sensitive to the redox state of the copper atoms and the coordination of the other ligands) and the marked energetic preference of the Pa_C state over other alternative PA structures studied have served as further evidence for the structural assignment of the Pi_C mode to the PI. All six models included a water molecule, which is hydrogen-bonded to the T3 bridging OH^- ligand (if present). In the nomenclature adopted in ref 21, the six model systems are Ox = Ox{ OH^- , OH^- }, Pi_C = Pi{ H_2O , O_2^{2-} : C_3 }, Pi_S = Pi{ H_2O , OH^- , HO_2^- : S_{23} }, Pa_C = Pa{ H_2O , O_2^{2-} : C_3 }, Ni_C = Ni{ H_2O , OH^- , O^{2-} : C }, and Ni_S = Ni{ H_2O , OH^- , OH^- : S_{23} , OH^- : S_{23} }.

The coordinates of these models and the most plausible protonation states were taken from our previous QM/MM optimizations.

(40) (a) Krishnan, R.; Binkley, J. S.; Seeger, R.; Pople, J. A. *J. Chem. Phys.* **1980**, *72*, 650–654. (b) Clark, T.; Chandrasekhar, J.; Spitznagel, G. W.; Schleyer, P. v. R. *J. Comput. Chem.* **1983**, *4*, 294–301.

(41) Schäfer, A.; Huber, C.; Ahlrichs, R. *J. Chem. Phys.* **1994**, *100*, 5829–5835.

(42) Hehre, W. J.; Radom, L.; Schleyer, P. v. R.; Pople, J. A. *Ab initio molecular orbital theory*; Wiley-Interscience: New York, 1986.

(43) Because we have used the unrestricted Kohn-Sham (KS) formalism, the resulting KS determinants are not eigenfunctions of the \hat{S}^2 operator. While the deviation from the pure $S = 3/2$ (or $S = 1$ for peroxy) states is negligible for the ferromagnetically coupled states, the antiferromagnetically coupled states deviate significantly from pure $S = 1/2$ (or $S = 0$) states, which can only be described by multireference wave functions. Nevertheless, this approach is routinely used in the studies of antiferromagnetically coupled model complexes representing metal sites in proteins. The reported values are unrestricted DFT energies without spin projection. The broken-symmetry technique can be used to correct the energies of the antiferromagnetically coupled (AF) states, viz. $E_{\text{AF}} = E_{\text{F}} - 3/2(E_{\text{F}} - E_{\text{BS}})$ for all three coppers coupled and $E_{\text{AF}} = E_{\text{F}} - 2(E_{\text{F}} - E_{\text{BS}})$ for two coppers coupled (e.g., peroxy intermediate), where E_{F} and E_{BS} are the energies of the ferromagnetically coupled state and the broken symmetry solution of the AF state, respectively, whereas E_{AF} is the corrected energy of the AF state.

(44) Noodleman, L.; Peng, C. Y.; Case, D. A.; Mouesca, J.-M. *Coord. Chem. Rev.* **1995**, *144*, 199–244.

(45) Sundaram, U. M.; Zhang, H. H.; Hedman, B.; Hodgson, K. O.; Solomon, E. I. *J. Am. Chem. Soc.* **1997**, *119*, 12525–12540.

Table 1. Calculated Doublet–Quartet (Singlet–Triplet for PI) Energy Gaps for the Six Studied Models Complexes of the MCO Trinuclear Active Site^a

system	$\Delta E_{\text{LS-HS}}$		
	protein ^b	imidazole ^c	NH ₃ ^d
NI _C	38.3	42.2	33.2
NI _S	25.9	25.1	29.0
Ox	18.6	17.9	12.5
PI _S	43.7	44.0	49.1
PI _C	-14.0	-13.5	-13.9
PA _C	26.5	23.9	26.8

^a All values are in kJ·mol⁻¹. A positive value indicates that the low-spin state is more stable. ^b QM/MM energy difference between low-spin (LS) and high-spin (HS) states. ^c In vacuo energy difference between HS and LS (at QM/MM geometries). ^d In vacuo energy difference between HS and LS, with NH₃ groups instead of imidazoles used to model copper-binding histidine residues.

However, all atoms in the imidazole groups were deleted except the donor nitrogen atoms and three hydrogen atoms were added. Therefore, the Cu–N distances are identical for those in the QM/MM optimizations, whereas, for the N–H bonds and the H–N–H angles, standard equilibrium values for ammonia ligated to divalent ions were used, viz 1.026 Å and 105.7°. ⁴⁶

3. Results and Discussion

3.1. Relevance of Model Systems. The first question to be answered is whether spectroscopic parameters, calculated in vacuum on small truncated models with NH₃ representing the His ligands, reproduce those that would be calculated (if feasible) or measured experimentally for the whole protein. We have considered this question by calculating the energy difference between the two lowest spin states of the six considered model complexes (singlet and triplet states for the PI and the ferro- and antiferromagnetically coupled quartet and doublet states for the other models). These calculations were performed with the DFT/BP86 method, either with the full QM/MM imidazole models in the protein (i.e., including a point charge model of the surroundings) or in vacuum or with the truncated NH₃ model in vacuum. The results in Table 1 show that the energy difference between the two spin states changes minimally (less than 4 kJ·mol⁻¹ in all cases and with a mean absolute difference, MAD, of 1 kJ·mol⁻¹) if calculated with the imidazole model in the protein or in vacuum. The effect of the replacement of imidazole with NH₃ is somewhat larger (up to 9 kJ·mol⁻¹; MAD 4 kJ·mol⁻¹). However, due to error cancellation, the most important comparison, imidazole models in the protein vs NH₃ ligands in vacuo, yields a maximum deviation of 6 kJ·mol⁻¹ and a MAD of 3 kJ·mol⁻¹. Thus, the effect of the truncation of the system on the spin splitting energies is small.

This finding is essential not only for the subsequent discussion but also for the verification of the recent experimental work^{19,20} that is based on the assumption that the studied inorganic model complexes (also with amine, rather than imidazole, ligands) reproduce the electronic and spectroscopic properties of the MCO intermediates in an accurate way. Also, it shows that the rather high charge (i.e., 3+ or 4+) of the model complexes does not significantly influence the spin-splitting energies as demonstrated by the comparison of in vacuo and QM/MM values (in which the

charge is compensated by at least two negative second sphere residues, viz. ref 21).

3.2. Character of the Electronic Ground States: Exchange Couplings. The recently published QM/MM structures of various alternatives for the intermediates in MCO catalytic cycle²¹ showed an excellent agreement with available EXAFS data and crystal structures. Moreover, the QM/MM energies of the various isomers strongly favored the PI_C coordination mode for PI (Figure 3e) and the NI_C mode for NI (Figure 3a). However, the triplet state was predicted to be the electronic ground state in disagreement with the experimental data for PI_C (cf., Table 1). This could be attributed to the inherent inaccuracy of current DFT functionals and the fact that single-determinantal methods yield broken-symmetry states ($M_s = 0$ in case of PI) rather than the pure spin states. While broken-symmetry methods have been widely used to deduce the sequence of pure spin states through mapping to Heisenberg Hamiltonians, it is desirable to rigorously calculate the multiplets of spin-coupled systems such as the present ones. This can be accomplished by multireference ab initio methods. Such methods are known to be computationally demanding. However, the case of three magnetically interacting Cu^{II} ions is relatively straightforward, because there are only three open-shells (three electrons in three orbitals) to be considered (vide infra). Therefore, state-specific CASSCF and CASPT2 calculations were carried out (see Table 4). These multireference methods correctly describe the electronic configurations of both low- and high-spin states and yield eigenfunctions of the $\langle S^2 \rangle$ operator. Since, to our best knowledge, no rigorous multireference treatment of trinuclear copper clusters has been reported before, we begin with the description of the character of the low- and high-spin wave functions for the intermediates.

As mentioned in the methods section, the Cu^{II}₃ system can as a first approximation be described by three electrons in three active orbitals. From this, the existence of one quartet (with the spin-function $|\alpha\alpha\alpha\rangle$) and two low-lying doublet configuration state functions (CSFs; one way to construct linearly independent and orthogonal spin-functions for this case is to choose $1/\sqrt{6}(-2|\alpha\alpha\beta\rangle + |\alpha\beta\alpha\rangle + |\beta\alpha\alpha\rangle)$ and $1/\sqrt{2}(-|\alpha\beta\alpha\rangle + |\beta\alpha\alpha\rangle)$) can be qualitatively predicted, but the energies of the electronic states arising from these CSF's can only be obtained from quantum chemical calculations (or from experiments). Indeed, the CASPT2/CASSCF-(27,15) calculations correctly predict a low-spin ground electronic state for all the six systems studied (cf., Table 4). Moreover, 12 orbitals in the active space remain almost doubly occupied in the first two doublet and the first quartet states. Thus, the three unpaired electrons that are responsible for the (anti)ferromagnetic exchange coupling between the centers are confined to the three orbitals depicted in Figure 4a for the model complex TrisOH (which is essentially a symmetric analogue of native intermediate in the NI_S binding mode). Moreover, in Figure 4b, the two partly occupied orbitals of the PI_C model are shown, to illustrate the dominant contribution to the antiferromagnetically coupled ground-state wave function of the PI.

It can be seen that low-lying doublet states in the TrisOH complex can be well described as a four-configuration

(46) Rulíšek, L.; Havlas, Z. *J. Am. Chem. Soc.* **2000**, *122*, 10428–10439.

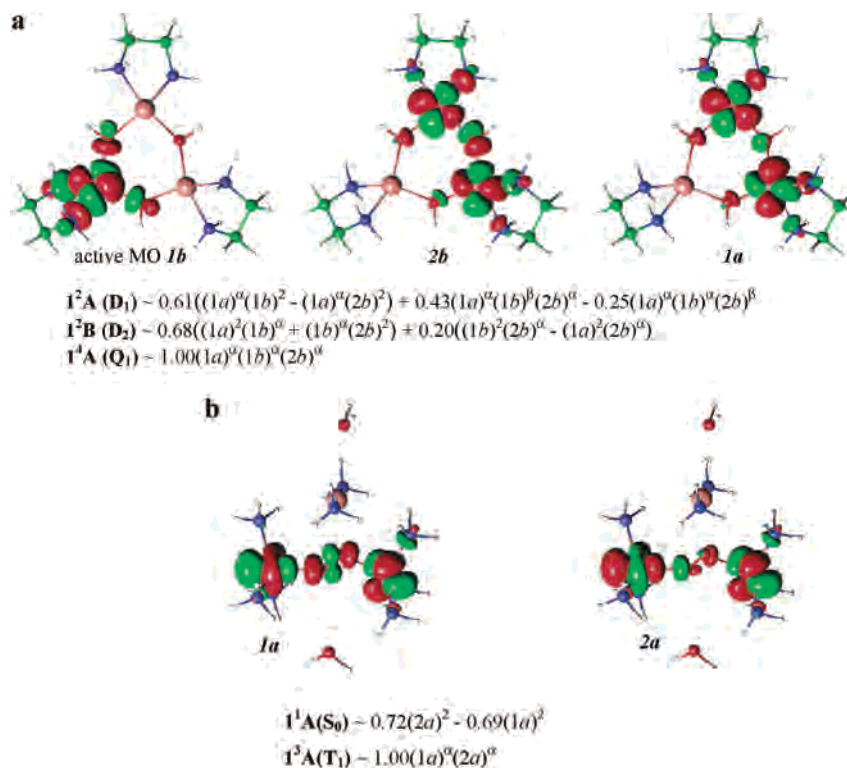


Figure 4. Visualization of the three partially occupied active orbitals in the TrisOH complex and the two partially occupied active orbitals for the PI binding mode of peroxy intermediate (together with the CI expansion coefficients). The $N^{2S+1}X$ term used in the figure denotes the N th state of a symmetry X and $(2S + 1)$ spin multiplicity.

problem, dominated (in both D_1 and D_2) by symmetric and antisymmetric combination of MOs composed mainly of copper d orbitals with a small contribution of ligand orbitals, as depicted in Figure 4a. For the PI (Figure 4b), it can be seen that the two orbitals responsible for the antiferromagnetic coupling have dominant contributions from the d orbitals of the two T3 Cu ions (presumably with dominant d_z^2 character) and the ground-state singlet is their antisymmetric combination. On the other hand, the wave functions for the high-spin states (triplets, quartets) have purely single-reference character.

3.3. Low-Lying Excited States and Zero-Field Splitting Parameters. Experimentally, a low-lying (150 cm^{-1}) excited doublet state has been observed for the NI,¹⁴ leading to the requirement of models in which all three Cu ions are directly bridged, either by a μ_3 -oxo group or by three OH^- bridges as in the NI_C and NI_S models, respectively. Calculations can provide a direct link to experimental values, because we can calculate the excitation energies of the second doublet state for two alternative binding modes of the NI (Figure 3a,b) and compare them with the spectroscopic observations.

Let us first assess the accuracy of the calculated values. To this aim, we have carried out calculations of doublet–quartet gaps and zero-field splitting parameters of the two inorganic model complexes that represent the two alternative binding models of the native intermediate and have been studied experimentally in detail: a 3-fold D_3 -symmetric trinuclear tris- μ_2 -hydroxy-bridged copper cluster (TrisOH)¹⁷ and a C_3 -symmetric μ_3 -oxo-bridged structure ($\mu_3\text{O}$), depicted in Figure 2.

The lowest quartet and the two lowest (degenerate) doublet states of TrisOH in D_3 symmetry are 4A_2 and 2E .⁴⁷ The 2E

state splits into two Kramers doublets by SOC.⁴⁸ A consistent value of the zero-field splitting (ZFS), $\Delta \approx 65\text{ cm}^{-1}$ (where Δ is a energy separation of the Kramers doublets), has been obtained experimentally.¹⁷ With RAS-SI calculations of the SOC between the nonrelativistic electronic states computed at the MS-CASPT2/CASSCF(27,15) level, we obtained $\Delta = 71\text{ cm}^{-1}$, in excellent agreement with the experimental data. The excitation energies of the SOC-perturbed states originating in the three lowest nonrelativistic states of each spatial and spin symmetry (i.e., 24 states in total) are summarized in Table 2.

In contrast, it has been found experimentally that the lowest electronic state of the μ_3 -O model system is quartet 4A , with the lowest doublet 2E lying 164 cm^{-1} higher in energy.²⁰ This is in excellent agreement with the calculated values of the doublet–quartet splitting in Table 3, which is 165 cm^{-1} without and 145 cm^{-1} with the inclusion of SOC. The calculations predict a ZFS for the lowest quartet state of $2D = -37\text{ cm}^{-1}$, which is somewhat larger than $2D = -5\text{ cm}^{-1}$ determined experimentally.¹⁹ It can be noticed that the sign of D can be estimated by observing that the relativistic ground state has $\sim 75\%$ character of the $S = 3/2$, $M_S = \pm 3/2$ state and $\sim 25\%$ of the $S = 3/2$, $M_S = \pm 1/2$ state, whereas the second state originating in the nonrelativistic 4A state has $\sim 75\%$ character of the $S = 3/2$, $M_S = \pm 1/2$ state and $\sim 25\%$ of the $S = 3/2$, $M_S = \pm 3/2$ state. The discrepancy of 32 cm^{-1} (0.4 kJ/mol^{-1}) between theory and experiment can be attributed to two factors: our computa-

(47) Tsukerblat, B. S. *Group Theory in Chemistry and Spectroscopy*; Academic Press: London, 1994.

(48) Tsukerblat, B. S.; Belinskii, M. I.; Fainzil'berg, V. E. *Sov. Sci. Rev. B Chem.* **1987**, 9, 337–481.

Table 2. Low-Lying Excited States of the TrisOH Model Complex^a

MS-CASPT2		SO-states	
state	ΔE	state	ΔE
1 ² A	0	1E _{1/2} ^b	0
1 ² B	27 ^c	2E _{1/2}	71
1 ⁴ A	196	3E _{1/2}	196
		4E _{1/2}	234
2 ² B	7931	5E _{1/2}	8173
3 ² B	7937	6E _{1/2}	8197
2 ² A	7954	7E _{1/2}	8217
4 ² B	8000	8E _{1/2}	8273
3 ² A	8029	9E _{1/2}	8314
4 ² A	8049	10E _{1/2}	8364
2 ⁴ A	8821	11E _{1/2}	9019
		12E _{1/2}	9093
1 ⁴ B	8850	13E _{1/2}	9143
		14E _{1/2}	9162
2 ⁴ B	10990	15E _{1/2}	11016
		16E _{1/2}	11186
3 ⁴ B	12031	17E _{1/2}	12362
		18E _{1/2}	12510
4 ⁴ B	19774	19E _{1/2}	20083
		20E _{1/2}	20147
3 ⁴ A	19831	21E _{1/2}	20179
		22E _{1/2}	20278
4 ⁴ A	22123	23E _{1/2}	22463
		24E _{1/2}	22471

^a The complex was studied in C_2 symmetry. Both nonrelativistic MS-CASPT2(27,15) energies of doublet and quartet states and relativistic-SOC corrected-energy values are listed. All values are in cm^{-1} . ^b All the relativistic states belong to the irreducible representation $E_{1/2}$ of the double group C_2^2 . ^c Owing to limitations in CASPT2 procedure in MOLCAS, we had to use the largest Abelian subgroup of D_3 symmetry (C_2). This results in the splitting of degenerate 2E ground state into a 2A and a 2B states, which split by 27 cm^{-1} at the MS-CASPT2 level. This is an artifact of higher states entering the state-averaged calculations. This can be demonstrated by state-specific CASPT2 calculations that give a splitting of 0.1 and 4 cm^{-1} between 2A and 2B states at the CASSCF and CASPT2 levels, respectively.

Table 3. Low-Lying Excited States of the $\mu_3\text{O}$ Model Complex, Assumed To Attain C_s Symmetry^a

MS-CASPT2		SO-states	
state	ΔE	state	ΔE
1 ⁴ A''	0	1E _{1/2}	0
		2E _{1/2}	37
1 ² A'	164	3E _{1/2}	145
1 ² A''	165	4E _{1/2}	174
2 ² A''	8296	5E _{1/2}	8365
2 ⁴ A''	8346	6E _{1/2}	8438
		7E _{1/2}	8484
3 ² A''	8358	8E _{1/2}	8538
2 ² A'	8416	9E _{1/2}	8619
3 ² A'	8456	10E _{1/2}	8692
3 ⁴ A''	8705	11E _{1/2}	8901
		12E _{1/2}	9119
1 ⁴ A'	14571	13E _{1/2}	14739
		14E _{1/2}	14791
2 ⁴ A'	15892	15E _{1/2}	15998
		16E _{1/2}	16035
3 ⁴ A'	24048	17E _{1/2}	24201
		18E _{1/2}	24238

^a Both nonrelativistic MS-CASPT2(27,15) energies of doublet and quartet states and relativistic-SOC corrected-energy values are listed. All values are in cm^{-1} .

tional protocol based on state-averaged CASPT2 calculations that has been used throughout this work (see footnote of Table 2) and the fact that we have enforced C_s symmetry onto the C_3 -symmetric $\mu_3\text{O}$ complex, which was necessary to make the CASPT2 calculations feasible (since no Abelian

subgroup of C_3 other than C_1 exists). The latter effect can be estimated to be $5\text{--}10 \text{ cm}^{-1}$ from Table S2, where both C_s and C_3 symmetric $\mu_3\text{O}$ complexes were studied with the less expensive MRDDCI2 method.

We conclude that very good agreement has been achieved between the computed and experimentally determined values for the splitting of the 2E state in TrisOH complex and quartet–doublet gap in $\mu_3\text{O}$ complex. This gives us a confidence in our calculated excitation energies of the intermediates in the reaction cycle of MCO, which are summarized in Tables 4 and 5.

First, we note that, in all cases, the low-spin state (i.e., singlet for PI and doublet for the rest of the systems) is the ground state. The quartets (or triplets for PI) come quite close in energy, $212\text{--}837 \text{ cm}^{-1}$. In particular, the calculated small singlet–triplet gap (348 cm^{-1}) for PI_C structure (the most likely candidate for the peroxy intermediate) is a plausible explanation for the incorrect prediction of the ground state in the DFT calculations,²¹ which has been a major problem in the assignment of this structure to the observed PI. Thus, we show here that the incorrectly predicted triplet ground state is indeed an anticipated shortcoming of DFT method rather than an inherent property of this structural arrangement.

For all Cu^{II}_3 systems, the second excited-state is also a doublet. Owing to the small excitation energies ($123\text{--}404 \text{ cm}^{-1}$), the doublets can be expected to be thermally populated at room temperature. On the other hand, such a low-lying state is not calculated for any of two PI structures, for which the second singlet states are found at 1360 and 7239 cm^{-1} , respectively. Experimentally, a $D_1\text{--}D_2$ splitting of $\sim 150 \text{ cm}^{-1}$ is observed for the NI.¹⁴ This is in a good agreement with the calculated values of 130 and 165 cm^{-1} for NI_C and NI_S, respectively. The quartet states are then calculated at 568 and 343 cm^{-1} above the doublet ground states, respectively (these values are obtained from CASPT2 calculations on top of state-specific CASSCF wave functions). To further increase the accuracy of the calculated values, we report (in Table 5) the SOC perturbed states for the two structural alternatives of the NI.

It can be seen that two D_2 states ($2E_{1/2}$) have excitation energies of 169 and 153 cm^{-1} , respectively, whereas the quartets splits into two doublets at ($428, 475$) and ($202, 220$) cm^{-1} . Therefore, it can be concluded that both structural alternatives are quantitatively consistent with the experimentally observed low-lying doublet state at $\sim 150 \text{ cm}^{-1}$, whereas the NI_C binding mode is in better agreement with the experimental estimate (obtained by magneto–structural correlation analysis) of a quartet state²¹ at $-3J \approx 780 \text{ cm}^{-1}$ (calculated at 568 cm^{-1}).

An interesting observation can be made when comparing the $\mu_3\text{O}$ and NI_C structures. Assuming similar effects are exerted by the ligand field, the only difference in coordination geometry between the two complexes is the presence of the OH^- bridge between Cu_3 and Cu_3' copper ions in NI_C. Still, this perturbation is enough to change the ground state multiplicity from a quartet to a doublet (similar effect has been shown by lowering O^{2-} ion into Cu_3 molecular plane in $\mu_3\text{O}$; viz. ref 19). Therefore, care must be taken when comparing results acquired on structurally similar species or using them for the prediction of complex biomolecular structures.

Table 4. Calculated Excitation Energies of All the Studied Model Complexes Calculated by the MS-CASPT2(27,15) (or (28,15) in the Case of PI) Method^a

spin	state	NI _C	NI _S	Ox	PI _S	PI _C	PA _C
LS ^b	1	0	0	0	0	0	0
	2	130	165	404	7239	1360	123
	3	10113	9804	5876	9945	2069	4432
	4	10347	9819	5900	10074	2810	4459
	5	14199	11713	6226	12294	3440	18303
HS ^c	1 ^d	419 (568)	212 (343)	490 (491)	837 (796)	348 (279)	283 (178)
	2	10531	7759	5804	7133	1406	4440
	3	14423	9970	5835	9915	2224	18397
	4	14809	11722	11432	16607	3420	22608

^a All values are in cm⁻¹. ^b The low-spin state (LS) is singlet for PI and doublet for oxidized resting state, NI, and PA. ^c The high-spin state (HS) is triplet for PI and quartet for oxidized resting state, NI, and PA. ^d Values in parentheses are the results of state-specific CASPT2 calculations.

Table 5. Calculated (Relativistic) Excitation Energies of the Two Structural Alternatives for Native Intermediate with the Inclusion of Spin–Orbit Coupling, Calculated by RAS-SI/MS-CASPT2(27,15)^a

state	NI _C	NI _S
1E _{1/2}	0	0
2E _{1/2}	169	153
3E _{1/2}	428	202
4E _{1/2}	475	220
5E _{1/2}	10264	7797
6E _{1/2}	10493	7798
7E _{1/2}	10686	9829
8E _{1/2}	10691	9845
9E _{1/2}	14363	9996
10E _{1/2}	14579	9997
11E _{1/2}	14601	11748
12E _{1/2}	14965	11758
13E _{1/2}	14984	11759

^a All values are in cm⁻¹.

A short discussion can be devoted to methodological aspects of the reported calculations. The CASPT2 method used here is considered to be one of the most accurate of available methods that can be used for the study of systems of up to ~50 atoms. However, this method is relatively expensive and competing alternatives, such as TD-DFT (which is 1 or 2 orders of magnitude faster), are always considered as the methods of the first choice. In the Supporting Information (Table S1), we demonstrate that TD-DFT approach fails completely and does not predict any low-lying doublet states for Cu^{II}₃ clusters. The reason for this failure is simply the inability to describe the reference low-spin state, which is a broken-symmetry state in DFT, whereas it is a multiconfigurational state in a rigorous treatment. On the other hand, the more recently developed methods SORCI (spectroscopically oriented CI)²⁸ and the even simpler MRDDCI2 method²⁹ give results of accuracy comparable to that of CASPT2 (MRDDCI2 values are listed in Table S2) with the exception of the PI_C intermediate, for which the MRDDCI2 method predicts the singlet state to be slightly higher in energy than the triplet (by 21 cm⁻¹) and reverses the order of quartet and doublet states in the μ₃-O complex (by 37 cm⁻¹). However, given the extremely delicate balance of the spin state energetics studied, the small basis sets used, and the considerably reduced computational cost, the results should be considered very reasonable.

In conclusion, we recommend the methodology used here, i.e., CASPT2 calculations of the electronic spectrum at the QM/MM optimized protein geometries, or the much cheaper and only slightly less accurate MRDDCI2//QM/MM(DFT) variant.

3.4. Notes on the Reaction Cycle of MCOs. Previous experimental and computational studies have pointed out two possible modes for the binding of O₂ to the trinuclear Cu₃ cluster: in the center of the cluster or on the Cu₂–CuT₃ side, as are represented by the PI_C and PI_S models.^{11,21} All other alternatives, such as the apical binding of O₂ to any of the T₃ copper ions, are not even local minima on the QM/MM potential energy surface. Comparing the QM/MM energies for PI_C and PI_S,²¹ we predicted that the former binding mode of O₂ is more stable²¹ by ~80 kJ·mol⁻¹. Moreover, the structures of PI_C and PA_C are essentially identical (cf. Figure 3e,f), which is fully consistent with the experimentally observed similarity in most of spectroscopic characteristics.^{21,45} The remaining problem that prevented an assignment of the PI_C model to the observed peroxy intermediate has been the incorrectly predicted spin multiplicity of its electronic ground state at the DFT level (i.e., triplet state was lower in energy than singlet, in contrast to experiment). This problem is resolved here, as it is clearly shown by the more accurate multiconfigurational ab initio method (MS-CASPT2) that singlet state is the true ground electronic state of the PI_C model, and this finding is in agreement with the experimental observations.

Following the reaction path, the existence of a transient species, NI', has been postulated, which is probably formed by proton-coupled electron-transfer process. This transient species would be at the redox level of the NI, but the remaining two electrons needed for the cleavage of the O–O bond still reside on the copper ions (i.e., the cluster is in the Cu^{II}Cu^I₂ state and T₁ Cu is oxidized). The actual cleavage of the dioxygen bond and the formation of the NI is a two-electron process,¹⁴ and our calculations²¹ indicated that the peroxide needs to be protonated first, since the barrier for the cleavage of O₂²⁻ (unprotonated moiety) was too high.²¹ As has been shown here, both structural alternatives for NI, NI_C and NI_S, have a low-lying doublet state at ~150 cm⁻¹, whereas NI_C has a quartet state at 568 cm⁻¹, which is acceptably close to the experimental estimate of 780 cm⁻¹ (in NI_S, the quartet is predicted at 343 cm⁻¹). This, together with our previous energetic estimate that the binding arrangement in NI_C is ~140 kJ·mol⁻¹ more stable than that in NI_S,²¹ strongly indicates that NI_C is the correct model for the native intermediate in the reaction cycle of MCO. All the above arguments can be summarized in the graphical form of the MCO reaction cycle, schematically depicted in Figure 5, which is consistent with all available experimental

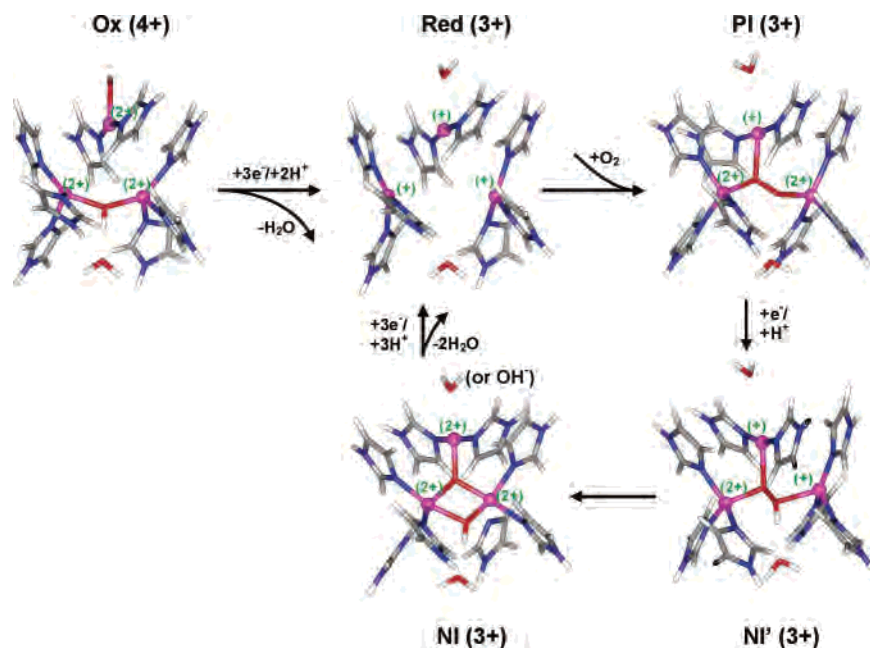


Figure 5. Structural model of the reaction cycle in MCOs, starting from the resting oxidized state, through the reduced state to the peroxy intermediate, then to the so-called NI' transient state (with one electron transferred from T1 Cu), and finally to the native intermediate.

observations^{11,14,20} as well as theoretical calculations (QM/MM modeling²¹ and this spectroscopic study).

Considering the spin patterns throughout the cycle, the triplet reactant (i.e., the singlet Cu_3 cluster with an incoming $^3\text{O}_2$ molecule) is immediately converted to a singlet state (PI) and the rest of the reaction occurs along the $S = 0$ or $S = 1/2$ low-spin surface (see also ref 49 for the role of antiferromagnetic coupling along the O_2 binding coordinate). This is probably an important factor for the overall reaction rate (the rate-determining step is the formation of the PI with $k \approx 2 \times 10^6 \text{ M}^{-1}\text{s}^{-1}$).

What remains to be understood in the reaction cycle of MCOs is the re-reduction of NI to the reduced state. This issue will be addressed in a forthcoming study.

4. Conclusions

In this work, we report the results of multireference calculations of spectroscopic parameters for model complexes representing the intermediates in the reaction cycle of the MCOs. To our best knowledge, this is the first study reporting rigorous multireference quantum chemical treatment of trinuclear copper complexes mimicking the active site in MCOs.

First, we have shown that the truncation of the model system from the protein into a small model site where imidazoles are represented by ammonia does not significantly influence the values of low-spin/high-spin energy splitting, which is an important finding both for the reported calculations and for the experimental work carried out for small inorganic models. Second, the character of the multireference electronic ground state of the studied Cu_3 clusters has been

analyzed, yielding insight into the nature of the wave function describing the bonding in these complexes. Third, excellent agreement between experimental data and theoretical calculations has been obtained for the inorganic TrisOH and $\mu_3\text{O}$ model complexes, which gives us confidence in our calculated data for the enzyme intermediates. Fourth, the calculations have allowed us to address the binding arrangements in the PI and NI states, and the results confirm our previous estimates which were based on energy arguments. In particular, the low-spin states were predicted as the ground states in all the intermediates studied as found experimentally. Fifth, a good agreement between theory and experiment is found for the lowest excited doublets of NI. Finally, a comparison of experiments and theory allows us to provide a detailed structural model for the reaction cycle of MCOs, which would have been difficult to achieve from either experiments or theory alone.

Acknowledgment. This work has been supported by grants from the Swedish Research Council, NIH DK-31450, LC512 (MSMT CR), and 203/05/0936 (GA CR). It has also been supported by computational resources from Lunarc at Lund University Computer Center. We thank Prof. Björn O. Roos and Dr. Mojmír Křiváňa for helpful discussions concerning the multireference (CASSCF and CASPT2) treatment of polynuclear metal centers and the relativistic effects (SOC) in quantum chemistry.

Supporting Information Available: The equilibrium geometries of all the studied molecules and TD-DFT and MRDDCI2 excitation energies for the six studied MCO intermediates. This material is available free of charge via the Internet at <http://pubs.acs.org>.

(49) Metz, M.; Solomon, E. I. *J. Am. Chem. Soc.* **2001**, *123*, 4938–4950.